*36th EPS Conference on Plasma Phys. Sofia, June 29 - July 3, 2009 ECA Vol.**33E**, O-2.003 (2009)*

Investigation on the relation between edge electric radial field asymmetries in RFX-mod and Greenwald limit

G.Spizzo, P.Scarin, M.Agostini, A.Alfier, F.Auriemma, S.Cappello, A.Fassina, P. Franz, R.Lorenzini, R.Paccagnella, L.Piron, P.Piovesan, I.Predebon, M.E.Puiatti, M.Valisa, N.Vianello, M.Zuin

Consorzio RFX, Euratom-ENEA Association, Padova, Italy

Outline In all major confinement devices (tokamaks, stellarators, spheromaks and reversed-field pinches - RFP), a density limit has been found (Greenwald and Sudo limits). Results summarized in [1] show that in the RFP high density does not cause a disruption, but a sequence of phenomena leading to the disappearance of quasisingle helicity (QSH)/Single Helical Axis (SHAx) [2], density increase, radiation condensation and fast resistive decay of the plasma current. In this paper we discuss the coherence of the magnetic ripple and its effect on test particle motion, and the impact of edge turbulent transport through "blobs". The competition between collisional and turbulent transport may be envisaged to rule the observed density limit.

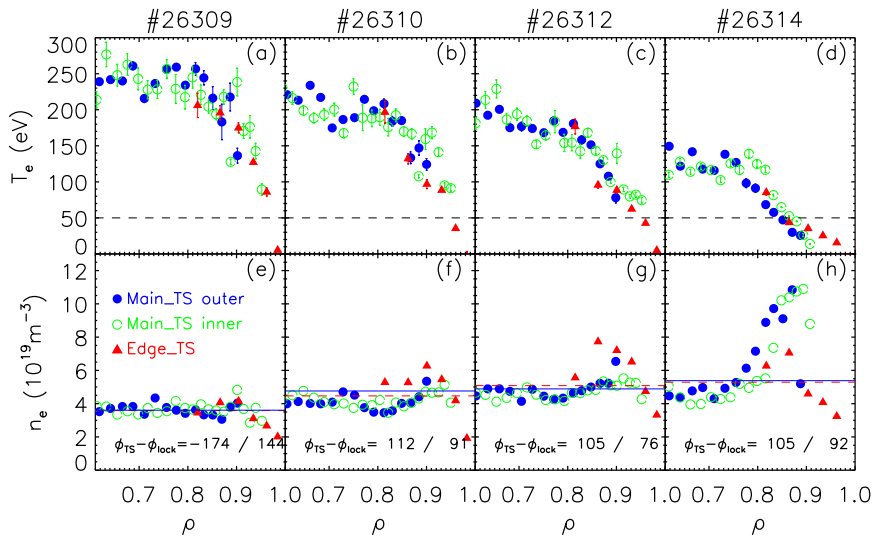

Figure 1: *TS profiles of temperature (a)–(d) and density (e)–(h) for a series of discharges with increasing n/n_G (left to right, $n/n_G = 0.28, 0.35, 0.44$ and 0.6). Dashed line in (a)–(d) marks $T_e = 50$ eV.*

Phenomenology In Fig 1 temperature and density profiles, measured by the main and edge Thomson Scattering (TS) diagnostics, are plotted as a function of the normalized poloidal flux coordinate $\rho = (\psi_p/\psi_{p,w})^{1/2}$ [1] in four different discharges with increasing density (normalized to the Greenwald density $n_G = I_P/\pi a^2$). Edge TS density profiles are calibrated absolutely, while those of the main TS are calibrated relative to the corresponding inverted interferometer profiles. There is an edge density increase, which is poloidally symmetric ($m = 0$, see the good matching between inner and outer main TS profiles) and toroidally localized at $\phi - \phi_{lock} \sim 100^\circ$, being ϕ_{lock} the toroidal position of the maximum coherent superposition of $m = 1$ MHD modes (often called "slinky" or

"locked mode"). By increasing n/n_G the "ring" expands towards the plasma core. As it is evident in Fig 1, the density increase is correlated with the widening of the radial region at low temperature (< 50 eV) where low ionization stages of impurities mainly emit. As explained in detail in [1], all these observations are likely explained by a radiative instability which increases resistivity and finally chokes the current. It is worth noting that the coherence of the $m = 0$ ripple increases as a function of n/n_G, as shown in Fig. 2 for the $m = 0$ phase dispersion parameter $\Delta^n = \varphi^{0,n+1} - \varphi^{0,n} - \varphi^{0,1}$ [3] ($\Delta = 0$ means maximum coherence).

In this respect, by exchanging poloidal and toroidal directions, the phenomenon of radiation condensation in RFPs resembles the MARFE in tokamaks [4]. Anyway, it is clear that the radiative instability is only the final outcome of a dynamical accumulation of density, toroidally localized and poloidally symmetric. Gas-puff imaging (GPI) [5] and internal system of sensors (ISIS) [6] blob toroidal velocity measurements v_ϕ show the presence of two null points: a source at $\phi = \phi_{lock}$ and a sink (stagnation point) at $\phi - \phi_{lock} \sim 100^\circ$ [the radial electric field averaged in the last 2-3 cm next to the wall, $\langle E_r(r,\phi)\rangle_r = v_\phi \cdot B_\theta$, corresponds to the GPI flow v_ϕ and is plotted as a solid blue line in Fig 3(e)]. The flow of blobs is (within a good approximation) the plasma flow itself [7]. We observe that the reversal of v_ϕ along the toroidal direction $\hat{\phi}$ conveys the edge robust toroidal flux ($\approx 10^{23}$ m^{-2} s^{-1}, much larger than the radial diffusive flux), to the stagnation point, where density accumulates, temperature decreases, resistivity increases and plasma emits radiation.

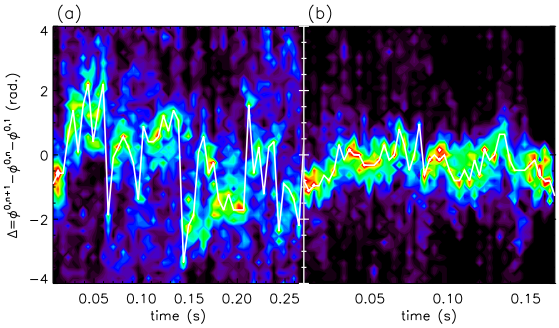

Figure 2: *Distribution of the $m = 0$ phase dispersion Δ^n, $n = 1-9$, as a function of time for two different discharges with (a) $n/n_G = 0.17$ and (b) 0.52*

Test particle simulations To study the modulation of E_r along ϕ, $\langle E_r(\phi)\rangle$, the Hamiltonian guiding center code ORBIT has been applied, using as input the eigenfunctions calculated from the Newcomb's equations in toroidal geometry [8]. Fig 3(e) shows the resulting Poincaré plot (toroidal angle ϕ as x-axis, ρ as y-axis) for a discharge with $n/n_G = 0.8$, at the time of the density peak. A chain of $m = 0$ islands is evident, with their O-points aligned in the vicinity of the unperturbed reversal (horizontal, dashed green line), and shifted outwards or inwards according to the toroidal modulation of ψ_p. At $\phi < \phi_{lock}$ the islands are pushed towards the wall (orange, dash-dot line in all frames), while at $\phi > \phi_{lock}$ they are shifted towards the axis.

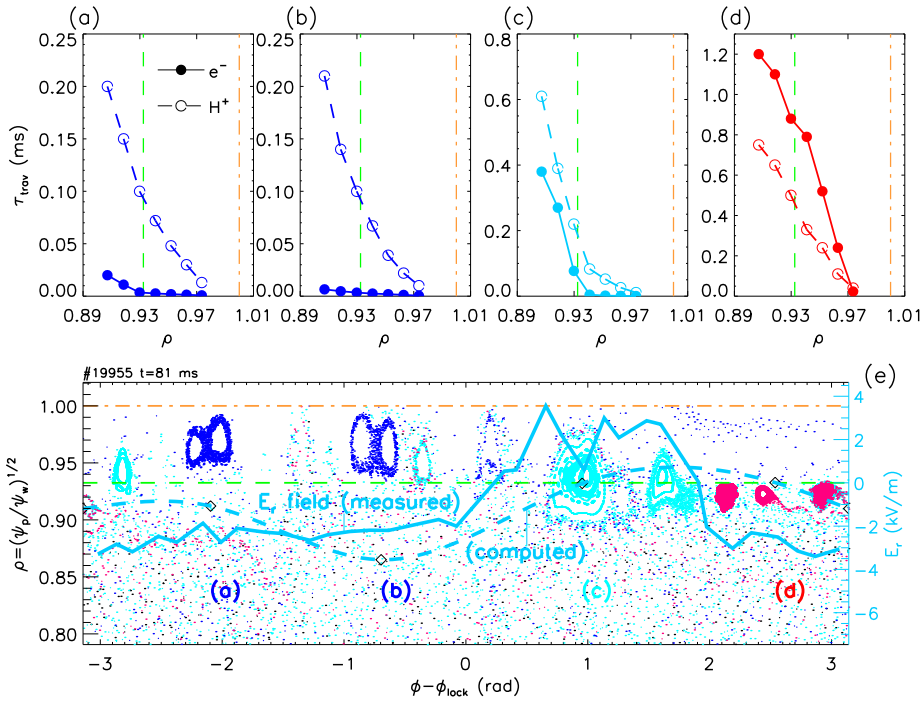

Figure 3: *(a)–(d): Travel times as a function of ρ for particles deposited at $\rho = 0.98$ and at toroidal angles corresponding to the labels (a)–(d) in frame (e); (e) Toroidal Poincarè plot with measured (solid) and computed (dashed) electric field.*

It is worth noting that the toroidal region marked by the letter (c) in Fig 3(e) is the region where the plasma flow (electric field) reverts its direction and density peaks as a consequence in region (d). It is therefore natural to study the radial motion of electrons and ions deposited near the wall and in the vicinity of the $m = 0$ islands marked by the letters (a)–(d) in the Poincaré plot. Before considering particle motions near the edge, ORBIT has been upgraded in order to take into account a recycling wall (in its standard configuration ORBIT has a perfectly absorbing wall). Particles are deposited at $\rho = 0.98$ and allowed to diffuse in any direction, under the action of magnetic field and collisions with the bulk ions/electrons. If particles hit the wall, they are bounced back by a gyroradius, and their pitch (normalized parallel velocity) $\lambda = v_{||}/v$ is re-initialized randomly. As an indicator of the radial transport we consider the "travel time" τ_{trav}, i.e. the time spent by 50%+1 particles to travel a prescribed radial distance from the initial deposition point. The travel times for electrons and ions are shown in Fig 3(a)–(d). Electron radial losses are much larger than ions in (a) and (b), since the "blue" islands [see Poincaré plot in Fig 3(e)] act as a short-circuit for their trajectories; ions are comparatively less mobile and reflect less the magnetic topology due to their larger drifts. As a consequence, a cloud of positive charges forms next to the wall, and as a result the ambipolar field would be directed inwards, which is the usual condition on the RFP [1]. This picture is changed only in the vicinity of the "red" islands in (d), where the magnetic topology is different: $m = 0$ islands are smaller, more conserved, topologically detached from the wall, and actually comparatively reduce the electron

mobility. As a consequence, $\tau_{\text{trav},e} > \tau_{\text{trav},i}$. If we make a rough estimate of the radial electric field required to balance the fluxes ($E_r = (\Gamma_e - \Gamma_i)/(\mu_i - \mu_e) \propto 1/\tau_{\text{trav},i} - 1/\tau_{\text{trav},e}$ if $\mu_e \gg \mu_i$) we obtain the dashed curve in Fig 3(e): this radial electric field is negative almost everywhere, except for a region at $\phi > \phi_{lock}$, and approaches the measured E_r.

Role of turbulence Since the convective toroidal flux nv_ϕ is always one order of magnitude larger than the diffusive terms [1], as soon as E_r reverts direction, there is density accumulation. A still open issue is why the reversal of E_r is seen experimentally in RFX-mod only when $n/n_G \gtrapprox 0.35$.

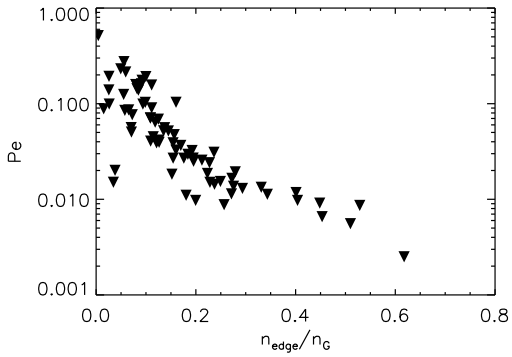

Figure 4: *Parameter $Pe = \tau_{e,i}/\tau_{tr}$ as a function of density divided by Greenwald density.*

We can note that the trapping process by blobs weakens as a function of collisionality. We define as an indicator the ratio $Pe = \tau_{e,i}/\tau_{tr}$ [9] between electron-ion collision time and transit time of blobs $\tau_{tr} = L_\phi/\tilde{V}$, being L_ϕ the toroidal dimension of blobs and $\tilde{V}$ the r.m.s. of v_ϕ, both measured by the GPI [7]. In Fig 4 we show *Pe* as a function of n_{edge}/n_G: this parameter falls off from 0.5 to 0.01 when $n/n_G \gtrapprox 0.35$, corresponding to a change from 2 to 100 electron-ion encounters per blob transit. This shows that at high density, collisions scattering particle trajectories are dominant in comparison to particle trapping within blobs, changing transport towards a Bohm-like scaling. This change in the diffusion regime could in principle have an impact in the edge radial transport that determines E_r.

References

[1] M. E. Puiatti, P. Scarin, G. Spizzo, M. Valisa, *et al.*, Physics of Plasmas **16**, 012505 (2009); M. E. Puiatti, P. Scarin, G. Spizzo, M. Valisa, *et al.*, Nuclear Fusion **49**, 045012 (9pp) (2009).

[2] M. E. Puiatti, this conference.

[3] P. Zanca *et al.*, Phys. Plasmas **8 (2)**, 516 (2001).

[4] B. Lipschultz, Journal of Nuclear Materials **145**, 15 (1987).

[5] M. Agostini, R. Cavazzana, P. Scarin, and G. Serianni, Operation of the gas-puff imaging diagnostic in the RFX-mod device, volume 77, p. 10E513, Rev. Sci. Instrum. (AIP), 2006.

[6] G. Serianni, W. Baker, and S. Dal Bello, High-spatial resolution edge electrostatic probe system for RFX, volume 74, pp. 1558–1562, Rev. Sci. Instrum. (AIP), 2003.

[7] P. Scarin, M. Agostini, R. Cavazzana, F. Sattin, G. Serianni, M. Spolaore, and N. Vianello, Journal of Nuclear Materials **390-391**, 444 (2009).

[8] M. Gobbin, L. Marrelli, and R. B. White, Plasma Phys. Control. Fusion **51**, 065010 (14pp) (2009).

[9] M. Vlad, F. Spineanu, J. H. Misguich, and R. Balescu, Phys. Rev. E **61**, 3023 (2000).